

MAPK Signaling and Inflammation Link Melanoma Phenotype Switching to Induction of CD73 during Immunotherapy



Julia Reinhardt¹, Jennifer Landsberg^{2,3}, Jonathan L. Schmid-Burgk⁴, Bartomeu Bibiloni Ramis², Tobias Bald^{2,5,6}, Nicole Glodde^{1,2}, Dorys Lopez-Ramos^{2,5}, Arabella Young^{6,7}, Shin Foong Ngiow^{6,7}, Daniel Nettersheim⁸, Hubert Schorle⁸, Thomas Quast⁹, Waldemar Kolanus⁹, Dirk Schadendorf³, Georgina V. Long¹⁰, Jason Madore¹⁰, Richard A. Scolyer^{10,11}, Antoni Ribas^{12,13}, Mark J. Smyth^{6,7}, Paul C. Tumeh^{12,13}, Thomas Tüting^{2,5}, and Michael Hölzel¹

Abstract

Evolution of tumor cell phenotypes promotes heterogeneity and therapy resistance. Here we found that induction of CD73, the enzyme that generates immunosuppressive adenosine, is linked to melanoma phenotype switching. Activating MAPK mutations and growth factors drove CD73 expression, which marked both nascent and full activation of a mesenchymal-like melanoma cell state program. Proinflammatory cytokines like TNF α cooperated with MAPK signaling through the c-Jun/AP-1 transcription factor complex to activate CD73 transcription by binding to an intronic enhancer. In a mouse

model of T-cell immunotherapy, CD73 was induced in relapse melanomas, which acquired a mesenchymal-like phenotype. We also detected CD73 upregulation in melanoma patients progressing under adoptive T-cell transfer or immune checkpoint blockade, arguing for an adaptive resistance mechanism. Our work substantiates CD73 as a target to combine with current immunotherapies, but its dynamic regulation suggests limited value of CD73 pretreatment expression as a biomarker to stratify melanoma patients. *Cancer Res*; 77(17): 4697–709. ©2017 AACR.

¹Unit for RNA Biology, Department of Clinical Chemistry and Clinical Pharmacology, University of Bonn, Bonn, Germany. ²Laboratory of Experimental Dermatology, Department of Dermatology and Allergy, University of Bonn, Bonn, Germany. ³Department of Dermatology, University Hospital Essen, West German Cancer Center, University Duisburg-Essen, Essen, Germany. ⁴Institute of Molecular Medicine, University Hospital Bonn, University of Bonn, Bonn, Germany. ⁵Laboratory of Experimental Dermatology, Department of Dermatology, University of Magdeburg, Magdeburg, Germany. ⁶Immunology in Cancer and Infection Laboratory, QIMR Berghofer Medical Research Institute, Herston, Queensland, Australia. ⁷School of Medicine, University of Queensland, Herston, Queensland, Australia. ⁸Department of Developmental Pathology, Institute of Pathology, University of Bonn Medical School, Bonn, Germany. ⁹Molecular Immunology and Cell Biology, Life and Medical Sciences Institute, University of Bonn, Bonn, Germany. ¹⁰Melanoma Institute Australia and Sydney Medical School, The University of Sydney, Sydney, New South Wales, Australia. ¹¹Department of Tissue Pathology and Diagnostic Oncology, Royal Prince Alfred Hospital, Sydney, New South Wales, Australia. ¹²University of California Los Angeles (UCLA), Los Angeles, California. ¹³Jonsson Comprehensive Cancer Center, Los Angeles, California.

Note: Supplementary data for this article are available at Cancer Research Online (<http://cancerres.aacrjournals.org/>).

Current address for J.L. Schmid-Burgk: Broad Institute of MIT and Harvard, Cambridge, Massachusetts; and current address for P.C. Tumeh, Acteris, South San Francisco, California.

Corresponding Author: Michael Hölzel, Unit for RNA Biology, Department of Clinical Chemistry and Clinical Pharmacology, University of Bonn, Sigmund-Freud-Strasse 25, Bonn 53105, Germany. Phone: 4922-8287-12170; Fax: 4922-8287-12159; E-mail: Michael.Hoelzel@ukb.uni-bonn.de

doi: 10.1158/0008-5472.CAN-17-0395

©2017 American Association for Cancer Research.

Introduction

The treatment outcome of patients with metastatic melanoma has significantly improved in recent years. Small-molecule MAPK inhibitors (MAPKi) prolong survival by targeting oncogenic signaling of the mutant BRAF kinase (BRAF^{V600E}), which is found in about half of melanomas (1, 2). Antibodies against negative immune checkpoint molecules PD-1/PD-L1 (programmed death 1/programmed death-ligand 1) and CTLA-4 (cytotoxic T-lymphocyte-associated antigen 4) enforce antitumor immune responses and achieve long-term remissions (3). Adoptive T-cell transfer (ACT) therapy is another type of immunotherapy that effectively controls tumor growth by targeting specific tumor antigens (4–6). Nevertheless, many melanoma patients do not respond or acquire resistance to these therapies. Apart from genetically hardwired mechanisms (7–9), there is growing evidence that nongenomic changes drive a coordinated coevolution of the tumor and immune cell compartment, which contributes to treatment failure (10, 11). Therefore, understanding the reciprocal crosstalk between tumor and immune cells in the microenvironment is instrumental to optimize current treatments.

Cellular plasticity plays a central role in nongenomic resistance mechanisms and phenotypic heterogeneity in melanoma (12). This has been elaborated in the context of acquired resistance to MAPKi (13–15). Dysregulated expression of MITF (microphthalmia-associated transcription factor), the master transcription factor of the melanocyte lineage, has been found to alter drug responsiveness. In particular, loss of MITF was shown to confer MAPKi resistance by activation of compensatory

Reinhardt et al.

survival signaling through different mechanisms (13, 14). Low expression of MITF by melanoma cells has been linked to the so-called "invasive" phenotype switch, which is characterized by an epithelial-to-mesenchymal (EMT)-like transition with higher migratory capacity (16, 17). In contrast, the so-called "proliferative" phenotype is strongly driven by MITF, which controls melanocyte lineage gene expression. Recently, single-cell-based approaches provided evidence that melanoma cells exist in a phenotypic equilibrium, but the impact of driver mutations, and epigenetic and microenvironmental context remains to be determined (18, 19).

Comparatively little is known about dynamic phenotype changes of melanoma cells during immunotherapy. Using melanoma mouse models, we previously demonstrated that T-cell therapy-associated inflammation induces melanoma cell dedifferentiation, leading to therapy escape (20). Prolonged exposure of melanoma cells with proinflammatory cytokines like TNF α suppresses MITF and causes "invasive" phenotype switching. Low MITF expression causes a reciprocal activation of inflammatory pathways and instigates a feed-forward loop of chemokine expression promoting predominantly myeloid immune cell recruitment (21). Thus, melanoma phenotype switching rewires the tumor microenvironment with direct implications for cancer immunotherapy (12, 22). However, melanoma cell states other than the "invasive" and "proliferative" phenotypes remain poorly defined as well as the molecular mechanisms that govern transition.

Here we used a bioinformatic discovery approach to identify early molecular events in inflammation-induced melanoma cell plasticity. We found that expression of the immunosuppressive 5'ectonucleotidase CD73 marked both nascent and full activation of the EMT-like "invasive" melanoma cell state coordinated by the c-Jun/AP-1 transcription factor complex. We found upregulation of CD73 during immunotherapy in mouse and human melanomas. As CD73 generates immunosuppressive adenosine in the tumor microenvironment, our findings link melanoma phenotype switching to acquisition of immunosuppressive properties during immunotherapy. Our work supports the rationale of ongoing clinical trials (NCT02503774) that evaluate immune checkpoint inhibitors in combination with CD73 blockade (23).

Materials and Methods

Cell culture

Melanoma cells were cultured in a humidified incubator (5% CO₂, 37 °C) in RPMI1640 medium supplemented with 100 U/mL penicillin, 100 μ g/mL streptomycin, 2 mmol/L L-glutamine, and 10% FBS. All MaMel cell lines were established by D. Schadendorf (Essen, Germany) and provided to us between 2012 and 2013 (21). HcMel3 and HcMel3R cells were established between 2009 and 2012 by us from primary melanomas in HgfoxCdk4^{R24C} mice (20). MZ7 and SK-MEL28 cells were provided by T. Wölfel (Mainz, Germany) in 2010 (20). Oncogenic driver and other identifying mutations of the melanoma cell lines were revalidated by Sanger sequencing or NGS for authentication in our laboratory between 2009 and 2013. Virus was produced in HEK 293T cells (obtained from ATCC in 2009) cultured in complete DMEM medium. HEK 293T cells were authenticated by morphology and capability of virus production. All cell cultures were renewed at least every three months by rethawing of initial cryo stocks. All used cell lines were negative for mycoplasma and tested on a monthly basis by PCR. Reagents used were: 1,000 U/mL TNF α , 50

ng/mL HGF (Peprotech); 50 nmol/L trametinib (MEKi), 100 nmol/L SCH-772984 (ERKi), 1 μ mol/L BEZ235 (Pi3Ki/mTORi), or 1 μ mol/L MK-2206 (AKTi) (Selleckchem/Absource). Cells were treated daily with 5 μ mol/L 5-azacytidine (Sigma) for 6 days prior to stimulations.

Flow cytometry (FACS) analysis

A total of 2×10^5 cells were stained on ice in 50 μ L FACS buffer. Antibodies (all Biologend) used were: BV 421 anti-CD73 mAb 1:100 (clone AD2), biotin anti-mouse CD73 mAb 1:200 (clone TY/11.8), biotin rat IgG1 κ isotype control 1:200, BV 421 streptavidin 300 ng/mL. Twenty thousand events in the live cell gate were recorded on a FACSCanto II flow cytometer (BD Biosciences) and analyzed with FlowJo software.

Mice

C57BL/6 mice (H-2b) were purchased from Charles River. TCR-transgenic Pmel-1 mice expressing an $\alpha\beta$ TCR specific for amino acids 25–33 of human and mouse gp100 presented by H2-Db were bred as described previously (20). All animal experiments were approved by the local government authorities (LANUV, NRW, Germany) and performed according to the institutional and national guidelines for the care and use of laboratory animals.

ACT experiments

Groups of C57BL/6 mice were injected intracutaneously with 4×10^5 HcMel3 cells into the flanks. Nontreated (NT) mice were killed when tumors reached >10 mm in diameter. Mice were killed between 12 and 20 days after ACT start (early-during-treatment, EDT). Experiments were performed in groups of five and repeated twice. Late relapse (R) melanoma samples and cell lines have been described previously (20). ACT with Pmel-1 T cells and microarray gene expression analysis were carried out according to the MIAME guidelines as described previously (20, 22). Raw data are accessible through GEO (GSE40213, GSE71879, GSE99925). Details are described in Supplementary Methods.

Patients

Samples and clinical data were obtained with the approval of Institutional Ethics Committee boards (institutional review boards, IRB) and patients' consents at the respective clinical centers [UCLA/USA (UCLA IRBs 11-001918 and 11-003066), Sydney/Australia (Protocol No X10-0305 & HREC/10/RPAH/539)]. Patient studies were conducted in accordance with the ethical guidelines of the Belmont Report. For correlation of CD73 expression with clinicopathologic parameters, we retrospectively studied cases from melanoma patients and material was collected between January 1, 2000 and December 31, 2010. All patients had given their written informed consent in agreement and after approval by the local ethics committee of the University of Bonn (Bonn, Germany). Treatment and follow-up examinations were performed according to the recommendations of the German Society of Dermatology. Dacarbazine was the only approved systemic treatment for metastatic melanoma till 2011 at our institution (Department of Dermatology, University Hospital Bonn, Bonn, Germany). Patients with primary melanomas underwent surgical resection, which was largely curative. Nineteen of 126 of these patients had recurrent disease and received best supportive care or dacarbazine before death. One additional patient with recurrent disease was treated with a BRAF inhibitor. Four of the patients with cutaneous melanoma metastases were

treated with an immune checkpoint inhibitor (ipilimumab, nivolumab, pembrolizumab).

Immunohistology

Mouse melanomas were immersed in zinc-based fixative (BD Pharmingen) and human melanomas in buffered paraformaldehyde (DAKO). Paraffin embedding, hematoxylin and eosin stains and IHC were performed according to standard protocols (Supplementary Methods). Antibodies used were polyclonal rabbit anti-human CD73 antibody (Sigma HPA017357, 1:600, antigen-retrieval pH6 10 minutes) and rabbit anti-human CD14 mAb (Clone EPR3652, LifeSpan Bio Sciences, dilution: 1:25). Rabbit anti-CD73 mAb (clone D7F9A, #13160 Cell Signaling Technology, dilution 1:300, antigen-retrieval pH6 10 minutes) was used to detect mouse CD73 or human CD73 (Sydney cohort). Rat anti-mouse CD45 mAb (30-F11, BD Biosciences) was used to identify immune cells in mouse melanomas.

Gene regulation assays

qPCR, chromatin immunoprecipitation (ChIP)-qPCR, and CRISPR-Cas9 approach for gene regulation by conditionally expressed GFP-tagged transcription factors were performed as described previously (21). Used DNA oligos and protocol adjustment are described in Supplementary Table S1 and Supplementary Methods. For bisulfite conversion of 500 ng of genomic DNA the EZ DNA-Methylation Direct Kit (Zymo Research) was used according to the manufacturer's instructions. Used DNA oligos and NGS-based analysis are described in Supplementary Methods.

Immunoblots

Cells were lysed in Laemmli buffer and immunoblots performed according to standard procedures as described previously (21). Used antibodies are listed in Supplementary Methods.

Additional methods in detailed descriptions are found in Supplementary Methods.

Results

CD73 marks nascent "invasive" melanoma phenotype switching

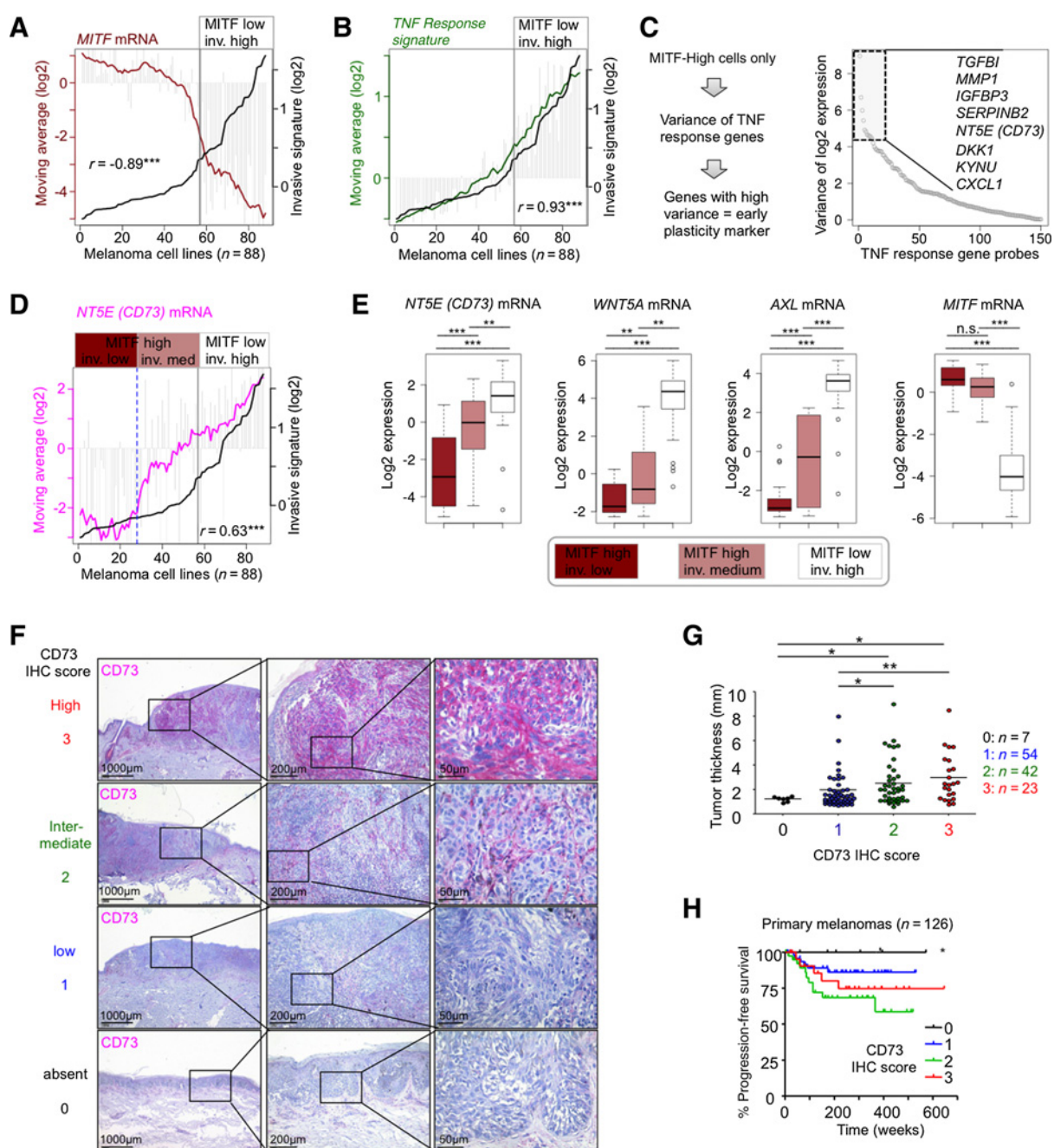
To identify markers and mechanisms of nascent "invasive" phenotype switching in melanoma, we used gene expression data from a well-characterized cell line panel ($n = 88$) (24). We ranked the cell lines by expression of the EMT-like "invasive" gene signature described by Verfaillie and colleagues (17) and analyzed the correlation with the expression level of *MITF* mRNA. This approach clearly separated *MITF*^{low} "invasive" melanoma cell lines from the others (Fig. 1A). Importantly, the "invasive" signature strongly correlated with our recently described melanoma TNF response signature (21), which supports the notion that inflammation-induced dedifferentiation and EMT-like "invasive" phenotype switching converge (Fig. 1B; ref. 25). Next, we searched for individual TNF response genes showing a high variance and thus a broad range of expression level in *MITF*^{high} cells. We hypothesized that high expression of such a gene in a *MITF*^{high} cell line could indicate intrinsic inflammatory pathway activation and nascent "invasive" phenotype switching (Fig. 1C). This analysis identified a small list of genes and among those, *NT5E* was of particular interest, because it encodes the 5'ectonucleotidase and mesenchymal stem cell marker CD73 (26–28). CD73 generates immunosuppressive adenosine in the microenvironment, which

defines the CD73-adenosinergic pathway as an emerging target for combination immunotherapy (29, 30). In comparison to the typical "invasive" phenotype markers *WNT5A* or *AXL* (13, 31), *NT5E* (*CD73*) showed robust expression in *MITF*^{high} cells with a nascent "invasive" phenotype as well as *MITF*^{low} cells with a fully established "invasive" phenotype (Fig. 1D and E). On the basis of this broad range expression of *NT5E* (*CD73*) in melanoma cell lines, we expected variable level of CD73 in human melanoma tissues. We established a protocol for sensitive and specific IHC detection of CD73 protein (Supplementary Fig. S1A and S1B) and we developed a CD73 IHC scoring system (0–3) to categorize CD73 expression level (Fig. 1F). In a cohort of primary cutaneous human melanomas with known sentinel lymph node status ($n = 126$), CD73 expression was significantly associated with tumor thickness, ulceration, and a positive sentinel lymph node (Fig. 1G; Supplementary Table S2). Most melanomas expressed a low or intermediate level of CD73 (Supplementary Table S2). Absence of CD73 expression (IHC score 0) was only found in thin melanomas, which had a better progression-free survival. Otherwise, we found no significant association between CD73 and progression-free or overall survival in patients with primary melanomas (Fig. 1H) or with cutaneous melanoma metastases ($n = 70$), respectively (Supplementary Fig. S1C). The distribution of CD73 IHC scores was comparable between primary melanomas and cutaneous melanoma metastases (Supplementary Fig. S1D; Supplementary Table S2). Taken together, CD73 showed variable expression in human melanomas, and gene signature analyses defined that *CD73* expression associated with both a nascent and fully established EMT-like "invasive" phenotype.

MAPK and proinflammatory signaling cooperatively induce CD73

Next, we searched for signaling pathways that enhance *CD73* expression and a nascent "invasive" phenotype in *MITF*^{high} melanoma cells (Fig. 2A). We used gene-set enrichment analysis (GSEA) and found signatures related to c-MET (rank#2), HGF (rank#11), and NF- κ B (rank#13) signaling among the top hits (Fig. 2B and C), as well as other gene sets related to mitogenic and proinflammatory signaling (Supplementary Table S3). The identification of NF- κ B signaling was confirmatory, because *CD73* is part of the identified melanoma TNF response signature (21) correlating with NF- κ B activity. HGF (hepatocyte growth factor) is the ligand for the receptor tyrosine kinase c-MET and a potent activator of MAPK and AKT signaling (32). Thus, this analysis suggested that mitogenic (e.g., HGF) and inflammatory signals (e.g., TNF α) cooperatively induce *CD73* expression and "invasive" phenotype switching. To test this hypothesis by functional studies, we used a panel of human melanoma cell lines with known driver mutation status (33). *CD73* protein expression was high in *MITF*^{low} but also several *MITF*^{high} cell lines (Fig. 2D), as predicated by our transcriptional analyses above and confirmed by FACS analyses (Fig. 2E, top). Negativity for CD73 in two of the tested cell lines could be explained by CpG island methylation in the promoter region of the *CD73* gene consistent with a previous study describing this mode of regulation (Fig. 2E, bottom; Supplementary Fig. S2; ref. 34). Of note, the two cell lines MaMel.71 and MaMel.15 without activating BRAF or NRAS mutations exhibited low levels of CD73 expression despite the lack of *CD73* promoter methylation. We hypothesized that this could be due to insufficient MAPK signaling. Indeed, HGF induced CD73 expression in both cell lines in a MEK-dependent

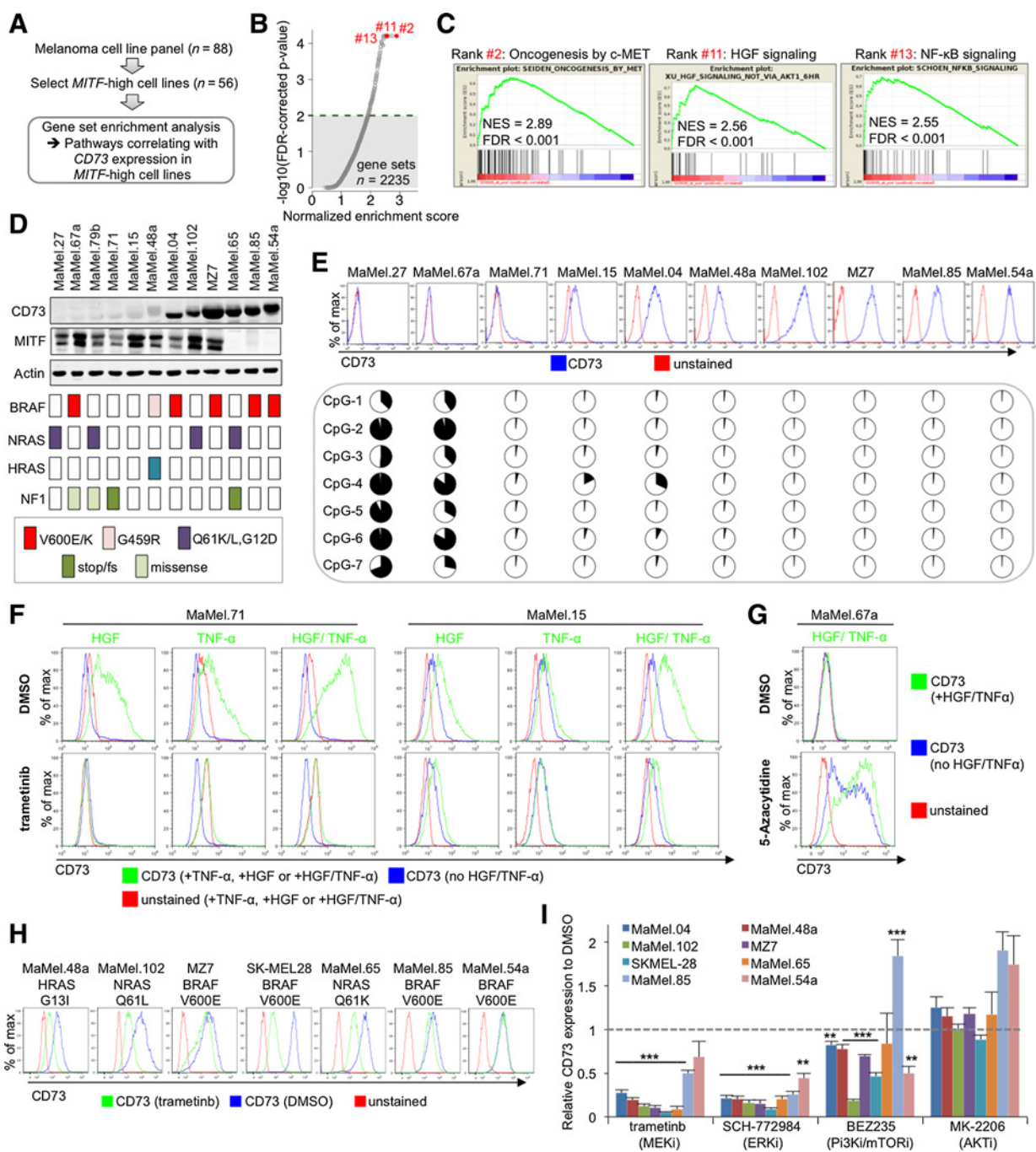
Reinhardt et al.

**Figure 1.**

CD73 marks both nascent and full activation of the "invasive" melanoma cell state program and shows heterogeneous expression in human melanomas. **A**, *MITF* log₂ expression of in melanoma cell lines ranked by Verfaillie "invasive" signature expression (17). Vertical gray bars indicate *MITF* expression in individual samples. Colored line indicates moving average. inv., invasive. **B**, Same as **A**, but for TNF response signature. **C**, Left, strategy to identify early plasticity marker. Right, variance of TNF response signature gene expression in *MITF*^{high} melanoma cells. **D**, Same as **A**, but for *NT5E (CD73)*. Dashed vertical line indicates median separation of *MITF*^{high} group by "invasive" signature expression. **E**, Expression of plasticity marker genes by melanoma cell subgroups. Two-sided unpaired *t* test with B&H correction (=false discovery rate). **F**, CD73 expression by IHC in primary human melanomas and scoring approach. **G**, Association of tumor thickness with CD73 IHC score in primary melanomas. Significance was determined by χ^2 test for categorical data ($P = 0.0028$) and analysis of variance by Kruskal-Wallis test ($P = 0.0025$). Asterisks indicate *P* values of group-wise comparisons after Dunn test to correct for multiple comparisons (false discovery rate). **H**, Survival analyses of patients with primary melanomas by CD73 IHC score. Log-rank test. *, $P < 0.05$; **, $P < 0.01$; ***, $P < 0.001$. n.s., nonsignificant.

manner and TNF α had a cooperative effect (Fig. 2F). Costimulation with HGF and TNF α enforced *MITF* downregulation (Supplementary Fig. S3A and S3B). In contrast, cell lines with *CD73*

promoter methylation (e.g., MaMel.67a) failed to upregulate *CD73* by HGF/TNF α costimulation, but became responsive upon prior exposure to the DNA-demethylating agent 5-azacytidine

**Figure 2.**

CD73 expression in melanoma cells is regulated by mitogenic and inflammatory signals in addition to promoter methylation. **A**, Outline of bioinformatic approach. **B**, Gene sets associated with CD73 expression in *MITF*^{high} cell lines. **C**, GSEA plots of top ranking gene sets. NES, normalized enrichment score; FDR, false discovery rate. **D**, Immunoblot analysis of melanoma cell line panel used in our study. Respective MAPK driver mutations are shown at bottom. **E**, CD73 expression by FACS in representative melanoma cell lines and corresponding promoter methylation status of CpG islands 1–7. Black color in pie charts represents the percentage methylated. **F–H**, CD73 expression by FACS in melanoma cells treated as follows: HGF, TNF α for five days (**F**); 6 days 5-azacytidine, then 3 days HGF/TNF α plus 5-azacytidine (**G**); trametinib for 4 days (**H**). Representative plots of biological triplicates are shown. **I**, *NT5E* (*CD73*) mRNA expression in melanoma cells lines treated as indicated for 4 days. Error bars indicate SD from three biological replicates. For statistical significance we compared *NT5E* (*CD73*) expression in each cell line in the presence of the inhibitor to the untreated DMSO control. Two-sided Student *t* tests with B&H correction (=FDR) for multiple comparisons. *, $P < 0.05$; **, $P < 0.01$; ***, $P < 0.001$.

(Fig. 2G). Finally, we dissected the contribution of different mitogenic signaling pathways to high CD73 baseline expression in the remaining cell lines. We found that the MEK inhibitor (MEKi) trametinib or the ERK inhibitor (ERKi) SCH-772984 suppressed CD73 protein and mRNA levels in most cell lines tested, in comparison with the Pi3K/mTOR inhibitor BEZ235 or the AKT inhibitor MK-2206 (Fig. 2H and I). Taken together, we found that MAPK signaling cooperates with the proinflammatory cytokine TNF α to induce CD73 in melanoma cells.

c-Jun/AP-1 induces CD73 expression via binding to an intronic enhancer

Next, we aimed to investigate the molecular mechanisms that control transcription of *CD73* in melanoma. We integrated ChIP-Seq data from the ENCODE database to identify transcription factors with reported binding in the *CD73* genomic region (Supplementary Table S4) that showed significant co-expression with *CD73* mRNA in melanoma cells. On the basis of this approach, the top ranking transcription factors were *IRF1*, *JUN* (*c-Jun*), and *NR3C1* (Fig. 3A). *JUN* was of particular interest, because others and we have recently shown that c-Jun/AP-1 is involved in melanoma phenotype switching (15, 17, 21, 35). c-Jun is a member of the heterodimeric AP-1 transcription factor complex that regulates cellular responses to mitogens, inflammation, and diverse stress conditions downstream of MEK-ERK and JNK signaling (36, 37). Classical heterodimerization partners of c-Jun are c-Fos, FOSL1 (FRA-1), and FOSL2 (FRA-2), which are also regulated by MEK-ERK signaling through transcriptional and posttranslational mechanisms. Thus, the AP-1 complex was a promising candidate to integrate mitogenic and inflammatory signaling in the regulation of *CD73* expression. Indeed, stimulation of MaMel.71 cells (BRAF^{wt}/NRAS^{wt}) with TNF α , HGF, or a combination of both led to cooperative induction of c-Jun (Fig. 3B). Accumulation of c-Fos and FOSL1 was largely dependent on HGF. To dissect the genomic context of *CD73* transcriptional regulation by the AP-1 complex, we aimed to use conditional gene expression approaches for *c-Jun*, because c-Jun can induce heterodimerization partners like FOSL1. Immunoblots confirmed the reciprocal expression of c-Jun and MITF in our melanoma cells as previously described (Supplementary Fig. S3C; refs. 13, 21). FOSL1 expression was notably lower in the two BRAF^{wt}/NRAS^{wt} cell lines MaMel.71 and MaMel.15, suggesting that lower MEK-ERK pathway activity impeded accumulation of FOSL1, as FOSL1 expression was dependent on MEK signaling in other cell lines (Supplementary Fig. S3D). Therefore, we reasoned that a CD73^{low} cell line with an activating BRAF or NRAS mutation (e.g., MaMel.79b) would be suitable for doxycycline-dependent conditional c-Jun expression. Interestingly, we found that a transient expression (achieved by low-dose doxycycline 25 ng/mL) of c-Jun tagged with the GFP variant citrine was sufficient to induce CD73, which persisted for several days (Fig. 3C). As MITF was only transiently suppressed, pulsed c-Jun expression established a MITF^{high}/CD73^{high} phenotype, which marks nascent activation of the "invasive" program. Having characterized this experimental system, we next looked for potential c-Jun/AP-1-binding sites in the *CD73* gene using ENCODE ChIP-Seq data (Fig. 3D). A ChIP-qPCR approach revealed prominent binding of c-Jun at the AP-1 sites #1–2 and #5–6 (Fig. 3E) coinciding with enhancer regions (H3K27Ac) identified by the ENCODE ChIP-seq project (Fig. 3D).

Next, we devised a CRISPR/Cas9 approach to clarify the functional relevance of the individual c-Jun/AP-1-binding sites.

MaMel.79b cells with inducible c-Jun were transiently transfected with Cas9-sgRNA constructs targeting these binding sites, as well as nearby control sites with no c-Jun/AP-1 motif. This was followed by CD73 induction through c-Jun, FACS analysis, and sorting of CD73^{low} versus CD73^{high} subfractions (lowest 10% versus highest 10% as unbiased cutoff) coupled to next-generation sequencing (NGS)-based analysis of mutagenesis frequencies at the respective c-Jun/AP-1 or control sites (Fig. 3F). We hypothesized that cells with successfully Cas9-mutagenized c-Jun/AP-1 sites should become enriched in the CD73^{low} subfraction and depleted from CD73^{high} subfraction if a particular AP-1-binding site was critical for CD73 expression. Strong enrichment of AP-1 site mutagenesis frequencies in the CD73 low subfractions (52% vs. 4% in CD73 lowest 10% vs. highest 10%) was observed only in the cell population transfected with the sgRNA against the c-Jun/AP-1 site #5 (Fig. 3G and H) being consistent with reduced CD73 surface expression (Supplementary Fig. S4A).

Next, we used the same approach to investigate whether the c-Jun/AP-1 site #5 was also driving high CD73 baseline expression in the melanoma cell lines SK-MEL28, MaMel.54a, and MaMel.85. Again, only targeting of the c-Jun/AP-1 site #5 resulted in a strong enrichment of the mutagenesis frequency in the CD73 low subfraction (73%) with a reciprocal reduction in the CD73 high subfraction (3%) considering a mutagenesis frequency of only 19% in the nonsorted total SK-MEL28 cell population (Fig. 3I). Similar results were obtained for MaMel.54a and MaMel.85 (Supplementary Fig. S4B). We then monitored CD73 surface expression in the total SK-MEL28 cell populations as well as FACS-sorted subfractions for several days (days 0, 3, and 7 after FACS sorting). This revealed a persistent reduction of CD73 surface expression only in the CD73 low FACS-sorted subfraction of cells transfected with the sgRNA against the c-Jun/AP-1 site #5 (Fig. 3J), being in line with the AP-1 site mutagenesis frequency of 73% (Fig. 3I). We corroborated this finding by showing a corresponding reduction of CD73 mRNA and protein level (Fig. 3K). Taken together, we identified a critical c-Jun/AP-1-binding site in an intronic enhancer of the *CD73* gene that controls its c-Jun/AP-1-dependent transcriptional activation downstream of mitogenic MAPK and inflammatory cytokine signaling.

CD73 is expressed in "invasive" and inflammatory mouse melanomas

We revealed multiple regulatory pathways for CD73 expression in human melanoma as a marker of tumor cell plasticity. Using mouse models, we previously dissected the interaction between inflammation and melanoma cell plasticity (20–22). Therefore, we aimed to investigate the regulation of CD73 in mouse melanomas with inflammation-driven tumor microenvironments. Recently, we described that *Braf*^{V600E}/*xCdk4*^{R24C} mice simultaneously develop amelanotic and pigmented melanomas (Fig. 4A; ref. 22). Amelanotic melanomas were infiltrated by myeloid immune cells (22) and this inflammatory microenvironment was also evident by broad chemokine gene expression (Fig. 4B). *CD73* mRNA level were significantly higher in inflamed amelanotic melanomas and coexpressed with typical "invasive" marker genes like *Axl*. Amelanotic *CD73*^{high} melanomas also exhibited higher levels of the AP-1 components *c-Jun* and *Fosl2* together with a reciprocal reduction of *Mitf* (Fig. 4C). GSEA using the hallmark gene set collection (38) showed elevated inflammatory (TNF α signaling) and mitogenic (KRAS signaling) pathway activity in amelanotic melanomas (Fig. 4D; Supplementary Table S5).

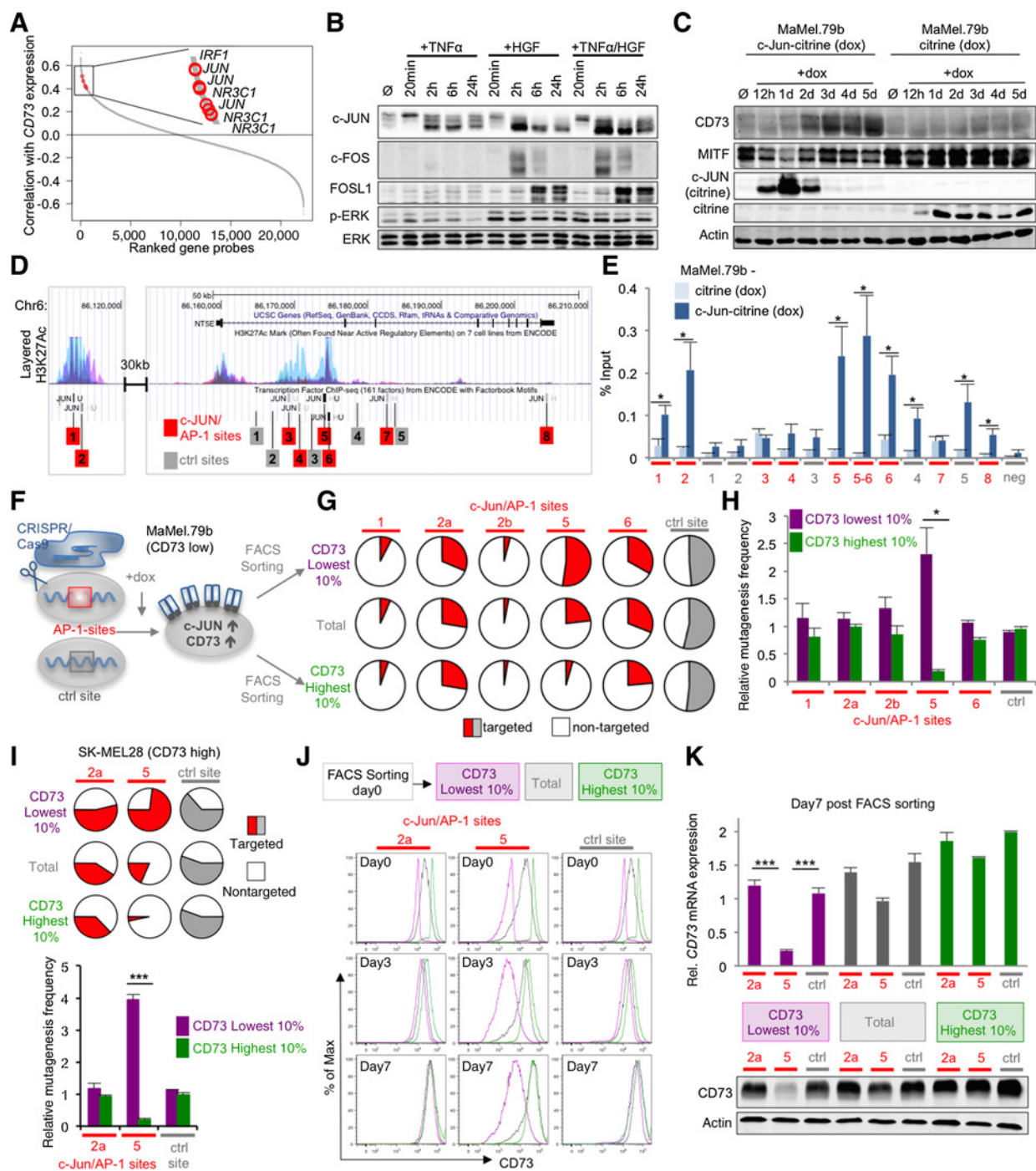
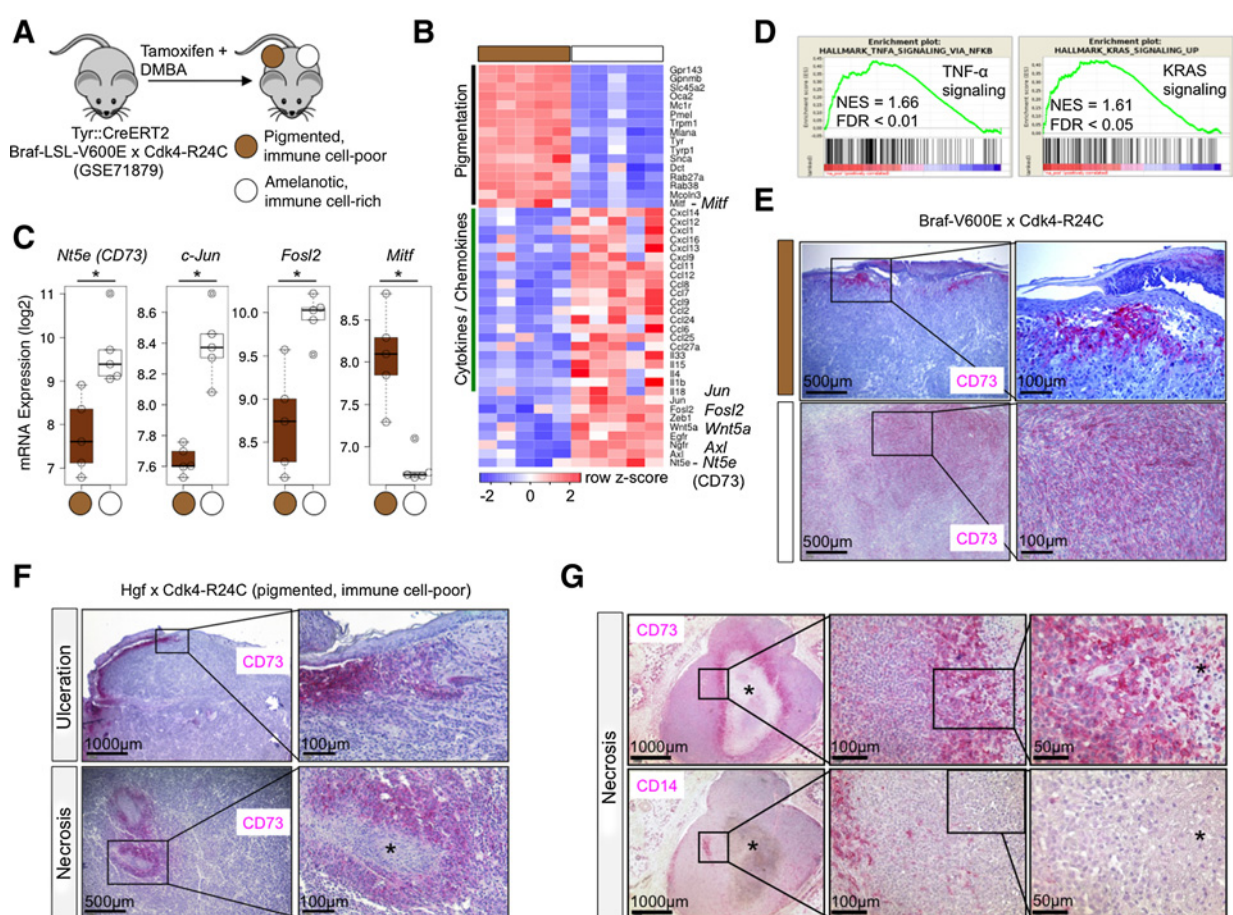


Figure 3.

c-Jun/AP-1 induces *CD73* in melanoma cells by binding to an intronic enhancer. **A**, ENCODE-annotated transcription factors binding at the *CD73* (*NT5E*) locus showing Pearson correlation > 0.4, with *CD73* (*NT5E*) mRNA expression in melanoma cell line. **B**, Immunoblots in MaMel.71 cells treated with TNF α (1,000 U/mL) and HGF (50 ng/mL) as indicated. **C**, Immunoblots in MaMel.79b conditionally inducing c-Jun-citrine or citrine by low-dose doxycycline (dox) stimulation. **D**, c-Jun/AP-1 binding sites in the *CD73* (*NT5E*) gene locus mapped by ENCODE. **E**, ChIP-qPCR tiling approach for c-Jun/AP-1 binding sites using MaMel.79b conditionally expressing c-Jun-citrine versus citrine as reference. Error bars indicate SEM of biological triplicates. One-sided *t* test for enrichment. **F**, Outline of the CRISPR/Cas9 approach. **G**, Pie charts showing c-Jun/AP-1 (red) or control site (gray) mutagenesis frequencies in FACS-sorted *CD73* lowest 10% versus highest 10% subfractions. **H**, Statistical analysis of relative AP-1 or control site mutagenesis frequencies corresponding to the experiment described in **F–G**. Error bars indicate SD from biological triplicates. Two-sided Student *t* test. **I**, Pie charts and statistical analysis of relative AP-1 or control site mutagenesis frequencies of FACS-sorted *CD73* lowest 10% versus highest 10% SK-MEL28 subfractions. Error bars indicate SD from biological triplicates. Two-sided Student *t* test. **J**, Monitoring of *CD73* surface expression by FACS in SK-MEL28 total cell populations and sorted subfractions transfected with the indicated sgRNAs. **K**, Quantifications of *CD73* mRNA and protein level by qRT-PCR and Western blot analysis in SK-MEL28 cell populations treated as described in **J**. Two-sided Student *t* test. *, *P* < 0.05; **, *P* < 0.01; ***, *P* < 0.001.

Reinhardt et al.

**Figure 4.**

CD73 expression in the spontaneous $Braf^{V600E}x Cdk4^{R24C}$ melanoma mouse model is linked to a mesenchymal phenotype and inflamed microenvironment. **A**, Summary of the model and datasets. **B**, Heatmap visualizing differential expression in pigmented versus amelanotic, immune cell-rich melanomas in $Braf^{V600E}x Cdk4^{R24C}$ mice. **C**, Boxplots showing expression levels of selected genes in phenotypically distinct melanomas. **D**, GSEA plots showing BROAD MSigDb hallmark gene sets associated with the amelanotic, immune cell-rich phenotype. NES, normalized enrichment score; FDR, false discovery rate. **E**, IHC for CD73 of $Braf^{V600E}x Cdk4^{R24C}$ mouse melanomas representative for the two different phenotypes. **F**, IHC for CD73 of $HgfxCdk4^{R24C}$ mouse melanomas with ulcerated and necrotic regions. **G**, IHC for CD73 and CD14 of human cutaneous melanoma metastasis with central necrotic area.

Immunohistochemical stains confirmed increased CD73 protein level broadly expressed throughout amelanotic $Braf^{V600E}x Cdk4^{R24C}$ melanomas, whereas CD73 expression in pigmented $Braf^{V600E}x Cdk4^{R24C}$ melanomas was localized and found at sites of ulceration or necrosis (Fig. 4E). This observation was recapitulated in pigmented primary melanomas from our related $HgfxCdk4^{R24C}$ mouse model (Fig. 4F). Human melanomas also showed intense CD73 expression around necrotic areas. In 32 of 70 (45.7%) human cutaneous melanoma metastases, necrotic areas could be detected and from that 23 of 32 (71.9%) showed intense CD73 expression around necrotic areas (Fig. 4G, top), which suggested hypoxia as another critical inducer of CD73 in melanoma. Indeed, hypoxia is known to promote "invasive" melanoma phenotype switching (39, 40) and drives CD73 expression in other cell types (41, 42). We also stained for CD14 to exclude that a potential recruitment of myeloid immune cells accounted for CD73 expression at the necrotic rim (Fig. 4G, bottom). In summary, the divergent phenotypic evolution of melanomas in the $Braf^{V600E}x Cdk4^{R24C}$ mouse model demonstrat-

ed that CD73 expression is linked to an inflamed and hypoxic microenvironment.

CD73 is induced in response to adoptive T-cell therapy

As cancer immunotherapy causes inflammation and damage in tumor tissues, we hypothesized that CD73 might be induced as part of an adaptive regenerative response (12). We have previously established an adoptive T-cell transfer (ACT) therapy that achieves remissions and long-term tumor control of primary $HgfxCdk4^{R24C}$ melanomas or transplantable HcMel3 melanomas (20). Adoptively transferred Pmel-1 CD8 T cells target the endogenous antigen gp100 (Pmel) expressed by melanoma cells. To study CD73 regulation and phenotypic coevolution under Pmel-1 T-cell therapy, we treated HcMel3 melanoma-bearing mice with our ACT protocol. Melanoma tissues were harvested for microarray gene expression analysis from mice early during ACT treatment (EDT, day 12–20 after ACT) and compared with nontreated (NT) controls and late relapse melanomas (R, day 140–210 after ACT; Fig. 5A; ref. 20). The induced antitumor immune response

following ACT was evidenced by the increase of *Cd8a* T cell and *Ifng* transcript level in EDT melanomas, which declined in relapse melanomas (Fig. 5B). In contrast, the myeloid marker transcript *Ilgam* (*Cd11b*) persisted in relapse melanomas, indicating a sustained myeloid immune cell infiltration.

Nt5e (*CD73*) mRNA expression was highest in relapse melanomas, but was already increased in EDT melanomas (Fig. 5B, right). We also confirmed high CD73 protein expression in relapse melanomas by IHC (Fig. 5C) and by FACS on isolated cell cultures from relapse melanomas (Fig. 5D). Careful histomorphologic analysis and stains for CD45⁺ immune cells also supported predominant CD73 expression by tumor cells in relapse melanomas *in situ* (Supplementary Fig. S5A and S5B). HcMel3-R cell lines also had moderately increased level of active phosphorylated ERK and AKT, but lacked expression of the melanocyte marker protein tyrosinase (Fig. 5E). Microarray gene expression analysis showed that inflammation-induced dedifferentiation and downregulation of pigmentation-related genes was progressive from EDT to relapse (Fig. 5F). This was accompanied by a reciprocal induction of "invasive" genes including *Axl* (Fig. 5F) and corresponding gene sets (Supplementary Fig. S6A).

Consistent with the decrease in CD8 T cells in relapse melanomas, we noticed a concomitant reduction of IFN targets (e.g., *Irf1*, *Irg1*, *Cd274*, *Iji205*) including genes encoding for MHC class II molecules and immunoproteasome components (*Psmb8*, *Psmb9*; Fig. 5F). GSEA also confirmed that ACT-induced IFN γ pathway activation in EDT melanomas (Fig. 5G top left; Supplementary Table S6) decreased in relapse melanomas (Fig. 5G, top right; Supplementary Table S7) in line with a diminishing anti-tumor T-cell response. In contrast, ACT-induced TNF α /NF- κ B pathway activation in EDT melanomas (Fig. 5G, bottom left; Supplementary Table S6) was not downregulated in relapse melanomas (Supplementary Table S7). We further found that lowered IFN γ pathway activity in relapse melanomas was associated with a reciprocal upregulation of cell-cycle-related gene sets including E2F (Fig. 5G, bottom right) and MYC (Supplementary Fig. S6B). Of note, the Verfaillie "proliferative" melanoma gene signature (17) was actually downregulated in relapse melanomas, because it largely contains MITF target genes including those involved in pigmentation or melanocyte differentiation (Supplementary Fig. S6B and S6C) and had almost no overlap with the E2F or MYC hallmark gene sets (Supplementary Fig. S6D). Importantly, inactivating mutations in the IFN γ pathway emerge as genetic determinants of primary and acquired resistance to checkpoint immunotherapy in melanoma patients (8, 9). Lowered IFN γ pathway activity in ACT relapse versus EDT mouse melanomas supported a critical role for IFN γ pathway inactivation in resistance. Furthermore, our findings defined that CD73 was preferentially induced in relapse melanomas. CD73 may facilitate therapy escape, as CD73-adenosinergic signaling limits immunotherapy in many solid cancer mouse models (30, 43–45).

Therefore, we asked whether we could find evidence for adaptive upregulation of CD73 in melanoma patients undergoing a similar type of ACT immunotherapy. In an independent study (Ribas and colleagues, manuscript in preparation), serial biopsies from six melanoma patients, which were treated and initially responded to adoptive transfer of MART-1 T-cell receptor transgenic lymphocytes and dendritic cell vaccination (NCT00910650; ref. 6), were screened for acquired loss of MART-1 (MLANA) and other melanocyte marker proteins. Indeed, one case (patient F5-1

in ref. 6) showed dedifferentiation with loss of the target antigen MART-1 upon progression. In this particular case, CD73 was reciprocally expressed and low before treatment, but induced upon MART-1 ACT therapy and persisted at progression (Fig. 5H), and thus similar to the relapse phenotype seen in our ACT-treated mouse melanoma model.

Dynamic regulation of CD73 in human melanomas during anti-PD-1 therapy

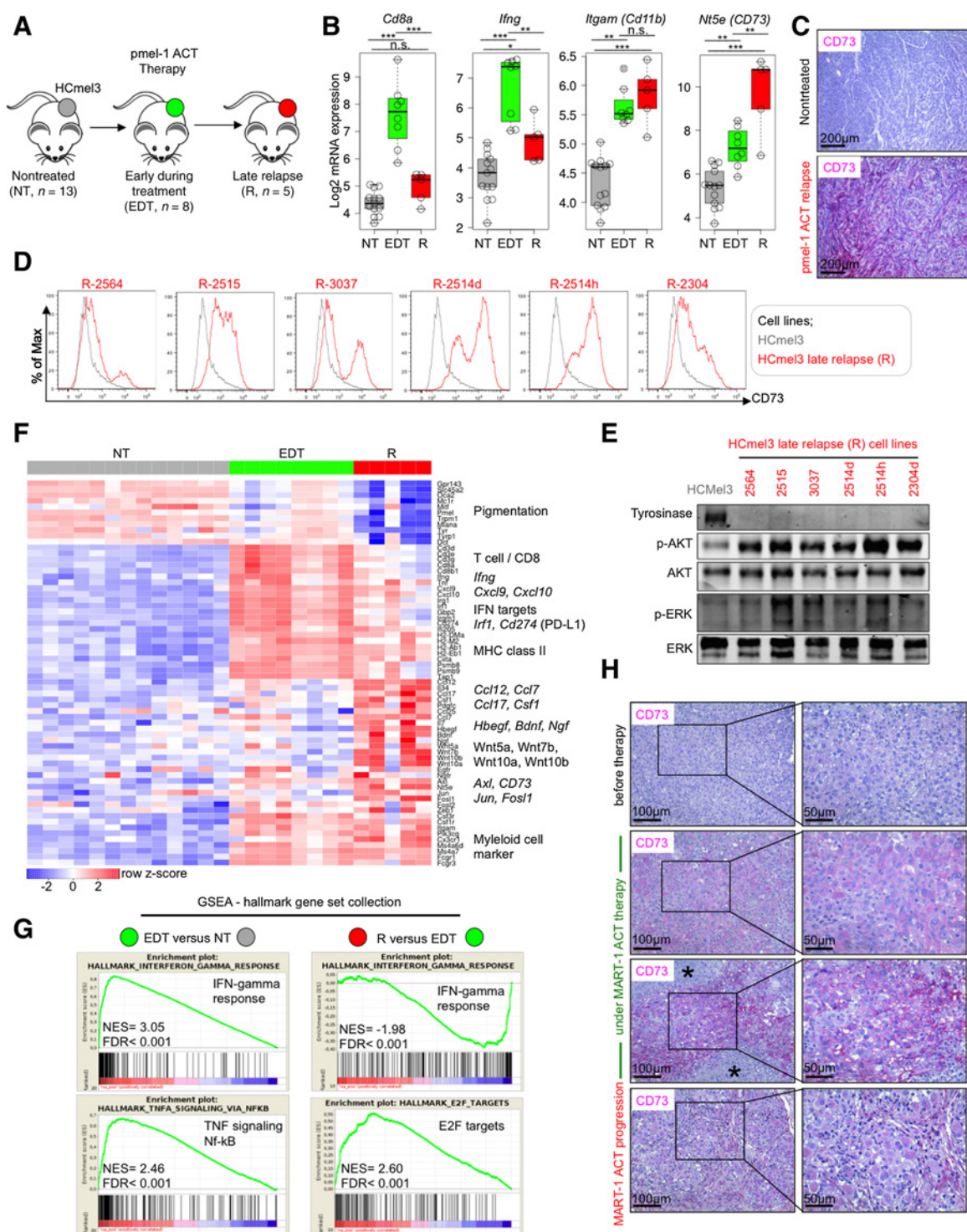
Next, we addressed whether dynamic regulation of CD73 also occurred in melanoma patients treated with checkpoint immunotherapy. Examining on-treatment biopsies from melanoma patients ($n = 25$, 16/25 cutaneous metastases, UCLA cohort) under pembrolizumab (anti-PD-1) therapy (46) revealed stable expression of CD73 in 13 cases (52%; Fig. 6A; Supplementary Table S8). In six cases (24%) all with a low CD73 baseline level (IHC score 1), we detected upregulation of CD73. In another six cases, of which three had highest CD73 baseline level (IHC score 3), we found downregulation of CD73. Notably, patients with progressive disease did not downregulate CD73, in fact the highest proportion of patients increasing CD73 displayed progressive disease (Fig. 6B). One case with a complete remission as best response showed upregulated CD73 in a recurrent lesion 306 days after start of anti-PD-1 treatment (Fig. 6C). We obtained similar findings in an independent cohort of melanoma patients ($n = 8$, Sydney cohort) treated with anti-PD-1 (pembrolizumab or nivolumab; Supplementary Table S9). Four cases were negative for CD73 expression across all longitudinal samples. Notably, three of these cases had received prior BRAFi+MEKi therapy. The remaining four cases had not received prior MAPKi therapy and were all CD73 positive at progression. Two of these cases demonstrated robust upregulation of CD73 at progression (case#7, acquired resistance; case#8 primary resistance; Fig. 6D and E). Together, dynamic upregulation of CD73 argues for an adaptive resistance mechanism and therefore CD73 blockade should not be restricted to melanoma patients with high CD73 expression in pretreatment biopsies.

Discussion

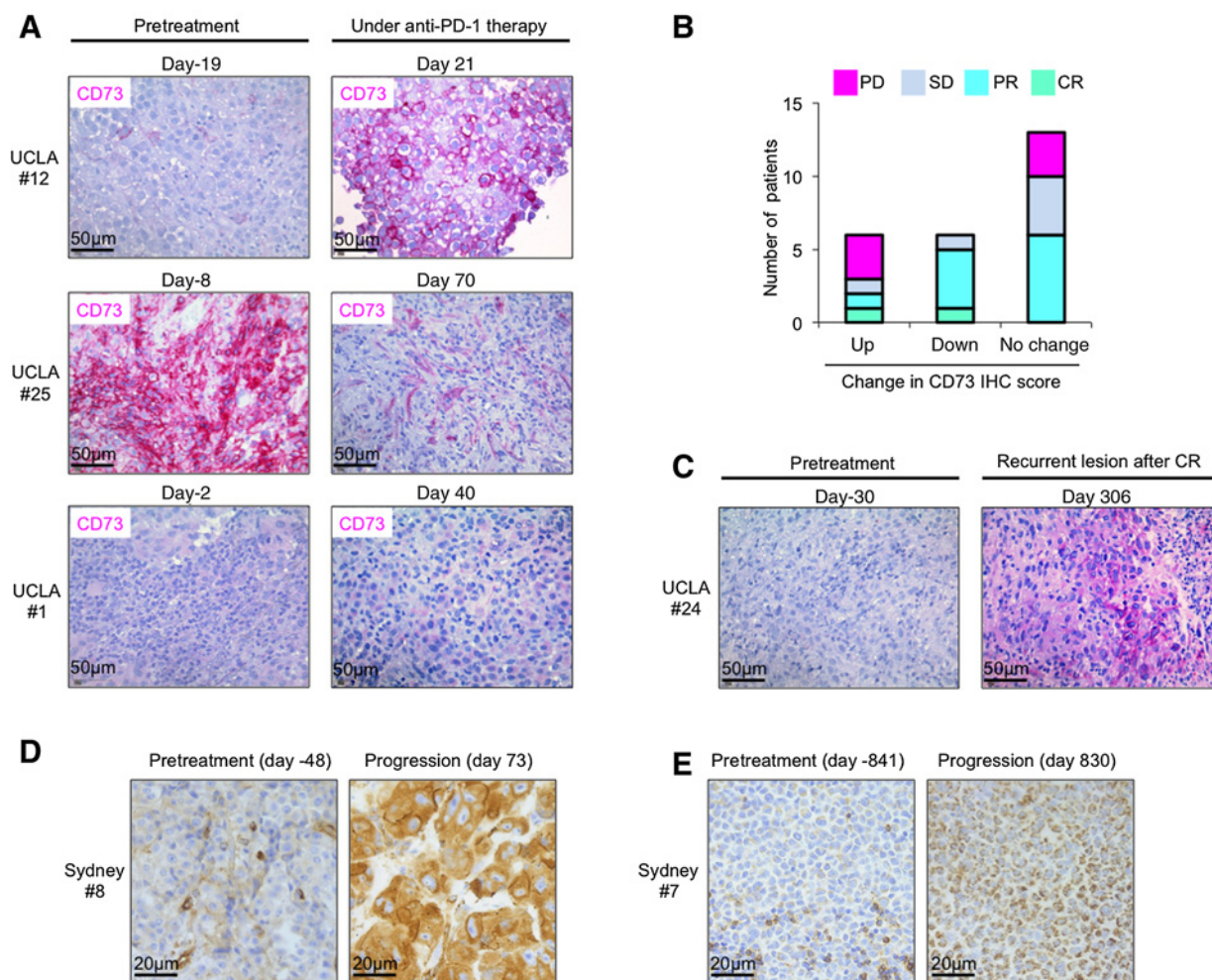
Here we identified the 5'-ectonucleotidase CD73 as a marker of melanoma cell plasticity. CD73 expression is associated with the EMT-like "invasive" phenotype, which is characterized by low expression of the melanocyte lineage transcription factor MITF (16, 17). Coexpression of CD73 with EMT markers in melanoma cells has been noted previously (47), but the mechanistic basis was not addressed. Importantly, we found that CD73 is strongly expressed by MITF^{low} but also by a subset of MITF^{high} melanoma cells, where it marks nascent activation of the EMT-like invasive program, which makes CD73 a distinct "invasive" marker (Supplementary Fig. S7). We demonstrated that MAPK signaling and the proinflammatory cytokine TNF α cooperatively induce CD73 expression through the c-Jun/AP-1 transcription factor complex, a central node in cellular stress signaling (36). This implements CD73 upregulation in a melanoma cell response to acute or chronic stress, which includes therapy-induced inflammation, hypoxia and amino acid starvation (12, 20, 48). Thus, CD73-adenosinergic signaling emerges as a stress-dependent regulator of melanoma phenotypes and immune cell interactions.

Our and the accompanying work by Young and colleagues show that MAPK pathway activity promotes CD73 expression, as

Reinhardt et al.

**Figure 5.**

CD73 induction during T-cell therapy is linked to melanoma phenotype switching in a regenerative microenvironment. **A**, Summary of available datasets. **B**, Boxplots for indicated mRNAs. n.s., nonsignificant; *, false discovery rate (FDR) < 0.05; **, FDR < 0.01; ***, FDR < 0.001; two-sided unpaired t test. **C**, IHC for CD73 of representative untreated and relapsed HCmel3 melanoma. Size bars indicate magnification. **D**, FACS for CD73 on HCmel3 and HCmel3 late relapse (R) cell cultures. **E**, Immunoblots for indicated proteins from cell lysates as shown in **D**. **F**, Heatmap visualizing changes in gene expression during pmel-1 ACT therapy of HCmel3 melanomas. **G**, Enrichment plots showing results of GSEA for indicated comparisons using the BROAD MSigDb hallmark gene set collection. NES, normalized enrichment score. **H**, IHC for CD73 of serial biopsies obtained from a melanoma patient (F5-1) treated within the MART-1 ACT trial (NCT00910650). Necrotic areas are indicated by asterisk (*). Size bars indicate magnification.

**Figure 6.**

Dynamic regulation of CD73 expression in melanomas from patients treated with anti-PD-1 therapy (pembrolizumab or nivolumab). **A**, Changes in CD73 expression by IHC shown in representative cases from the UCLA melanoma patient cohort ($n = 25$) treated with pembrolizumab. The clinical trial and the collection of serial biopsies was performed and described in a previous study (46). Biopsies were available from before and under pembrolizumab treatment. The corresponding CD73 IHC scoring is shown in Supplementary Table S8. **B**, Histogram showing the number of patients and their best objective responses separated by changes in CD73 IHC scores comparing CD73 expression before and under pembrolizumab treatment in melanomas from the UCLA patient cohort (total $n = 25$). Up, CD73 upregulation under pembrolizumab treatment. **C**, IHC for CD73 of melanoma biopsies from patient #24 (UCLA cohort) with a complete remission as best response showing high CD73 expression in a recurrent lesion 306 days after start of pembrolizumab treatment. **D** and **E**, IHC for CD73 of two cases with CD73 upregulation from the Sydney melanoma patient cohort treated both with pembrolizumab. The corresponding CD73 IHC scoring is shown in Supplementary Table S9. Scale bars indicate magnifications in IHC panels.

reported previously in A375 melanoma cells (49). In our concerted effort, we demonstrate that CD73 is downregulated in melanoma patients treated with MAPK inhibitors and sustained CD73 suppression correlates with a favorable response. MAPK-dependent regulation of CD73 has important implications for the development of treatment strategies, because combined inhibition of CD73 and A2A adenosine receptor (A2AR) has additional immunotherapeutic efficacy (30). Indeed, the accompanying work by Young and colleagues shows that MAPK inhibitors potentiate A2AR antagonism through CD73 downregulation.

Using our HcMel3 syngeneic inoculation model, we studied the phenotypic evolution of melanomas at different stages during adoptive T-cell therapy. CD73 was progressively induced and reached the highest level in dedifferentiated relapse melanomas

arguing that immunosuppressive CD73 facilitates therapy escape. As noted in our previous studies, mouse melanomas recapitulate phenotype transitions found in human melanomas (20–22, 50). Of note, EMT, hypoxia and wound-healing related gene signatures were shown to be upregulated in melanoma patients with poor response to anti-PD-1 therapy (11). Similar to our mouse models, we also found that CD73 was induced during MART-1 ACT or anti-PD-1 checkpoint immunotherapy in a subset of melanoma patients. Larger patient cohorts are needed to clearly define the relationship between CD73 modulation, treatment outcome and the type of resistance (primary versus adaptive). Cases with CD73 downregulation are of particular interest for future studies, because none of the patients in our limited cohort had a primary resistance.

Our experiments revealed downregulation of IFN γ signaling in mouse melanomas that escaped from Pmel-1 ACT therapy in line with a reduction of IFN γ -producing T cells at relapse. The reciprocal upregulation of proliferation-associated E2F/MYC gene signatures suggests that antiproliferative IFN γ signaling significantly contributes to immunotherapeutic efficacy. Previously, it was shown that IFN γ and TNF α released by infiltrating T cells promote senescence-like responses of tumor cells (51), and our analysis suggests that IFN γ signaling is critical for this senescence program. In support of this notion, inactivating mutations in the *JAK1/JAK2* kinases were recently identified in human melanomas with primary or acquired resistance to anti-PD-1 therapy (8, 9). *JAK1/JAK2* deficiency blocked IFN γ responses and conferred insensitivity to its antiproliferative effects. However, another report found that persistent IFN signaling activates an adaptive resistance program to checkpoint immunotherapy through the induction of several T-cell-inhibitory ligands including PD-L1 (52). These studies underscore that IFN γ signaling can exert opposing functions in the context of cancer immunotherapy and it remains to be investigated how this context dependency impacts on the CD73-adenosinergic pathway.

Combination immunotherapy is a strategy to limit primary or acquired resistance (53), but a better understanding of the tumor and immune cell crosstalk is needed (11). CD73-directed treatments also target inhibitory immune cells populations like regulatory T cells (27, 54, 55), which coevolve during immunotherapy. In melanomas, we showed that induction of immunosuppressive CD73 by mitogenic and inflammatory signals related to an EMT-like "invasive" phenotype as adaptive response to immunotherapy. As blocking CD73-adenosinergic signaling is effective in preclinical cancer models (30, 43, 44), our results support CD73 as a target to combine with current melanoma immunotherapies (23). This approach could restrain the production of immunosuppressive adenosine that may facilitate therapy escape. Finally, the dynamic induction of CD73 seen in subsets of melanoma patients during immunotherapy suggests that adjuvant CD73 blockade should not be restricted to patients with high CD73 expression in pretreatment biopsies. Measuring soluble CD73 (sCD73) in the blood of patients could help to identify cases with adaptive CD73 upregulation during immunotherapy. Our work has important implications for the development of biomarkers for anti-CD73 combination immunotherapies.

References

1. Cancer Genome Atlas Network. Genomic classification of cutaneous melanoma. *Cell* 2015;161:1681–96.
2. Robert C, Karaszewska B, Schachter J, Rutkowski P, Mackiewicz A, Stroiakovski D, et al. Improved overall survival in melanoma with combined dabrafenib and trametinib. *N Engl J Med* 2015;372:30–9.
3. Larkin J, Chiarion-Sileni V, Gonzalez R, Grob JJ, Cowey CL, Lao CD, et al. Combined nivolumab and ipilimumab or monotherapy in untreated melanoma. *N Engl J Med* 2015;373:23–34.
4. Rosenberg SA, Restifo NP. Adoptive cell transfer as personalized immunotherapy for human cancer. *Science* 2015;348:62–8.
5. Goff SL, Dudley ME, Citrin DE, Somerville RP, Wunderlich JR, Danforth DN, et al. Randomized, prospective evaluation comparing intensity of lymphodepletion before adoptive transfer of tumor-infiltrating lymphocytes for patients with metastatic melanoma. *J Clin Oncol* 2016;34:2389–97.

Disclosure of Potential Conflicts of Interest

G.V. Long is a consultant/advisory board member for Bristol-Myers Squibb, Amgen, Novartis, Merck, Roche, Pierre-Fabre, and Array. M.J. Smyth reports receiving a commercial research grant from Bristol Myers Squibb, Corvus Pharmaceuticals, and Aduro Biotech, is a consultant/advisory board member for Arcus Biosciences, has provided expert testimony for Corvus Pharmaceuticals. No potential conflicts of interest were disclosed by the other authors.

Authors' Contributions

Conception and design: J. Reinhardt, P.C. Tumeh, T. Tüting, M. Hölzel
Development of methodology: J. Reinhardt, J. Madore
Acquisition of data (provided animals, acquired and managed patients, provided facilities, etc.): J. Reinhardt, J. Landsberg, B.B. Ramis, T. Bald, N. Glodde, D. Lopez-Ramos, A. Young, S.F. Ngiow, D. Nettersheim, H. Schorle, W. Kolanus, G.V. Long, J. Madore, R.A. Scolyer, P.C. Tumeh, T. Tüting
Analysis and interpretation of data (e.g., statistical analysis, biostatistics, computational analysis): J. Reinhardt, J. Landsberg, J.L. Schmid-Burgk, B.B. Ramis, T. Bald, N. Glodde, A. Young, S.F. Ngiow, D. Nettersheim, T. Quast, W. Kolanus, D. Schadendorf, G.V. Long, J. Madore, R.A. Scolyer, A. Ribas, M.J. Smyth, P.C. Tumeh, T. Tüting, M. Hölzel
Writing, review, and/or revision of the manuscript: J. Reinhardt, J. Landsberg, T. Bald, N. Glodde, A. Young, S.F. Ngiow, H. Schorle, W. Kolanus, D. Schadendorf, G.V. Long, R.A. Scolyer, A. Ribas, M.J. Smyth, P.C. Tumeh, T. Tüting, M. Hölzel
Administrative, technical, or material support (i.e., reporting or organizing data, constructing databases): T. Bald, P.C. Tumeh, T. Tüting, M. Hölzel
Study supervision: M.J. Smyth, T. Tüting, M. Hölzel

Acknowledgments

We thank P. Aymans for managing the mouse colony, Sandra Ferring-Schmitt for help with dermatohistology, N. Fricker, K. Keppeler, S. Sivalingam, A. Heimbach for help with microarray and NGS (UKB Genomics & NGS Core Facility, Department of Human Genetics), E. Endel, P. Wurst and An. Dolf for help with FACS sorting (UKB FACS core facility).

Grant Support

M.J. Smyth was supported by National Health and Medical Research Council of Australia (NHMRC) Senior Research Fellowship (1078671) and Project Grant (1120887). J.L. Schmid-Burgk was supported by the German Academic Scholarship Foundation. T. Bald was funded in part by an EMBO Long-Term Fellowship (ALTF 945-2015) and the European Commission (Marie Curie Action LTFCOFUND2013, GA-2013-609409). This research was funded in part by grants from the DFG (TU 90/8-1, A22 in the SFB704 and A27 in the SFB854; to T. Tüting) and in part by grants from the Deutsche Krebshilfe (111084 to M. Hölzel) and DFG (HO4281/2-1 to M. Hölzel).

The costs of publication of this article were defrayed in part by the payment of page charges. This article must therefore be hereby marked *advertisement* in accordance with 18 U.S.C. Section 1734 solely to indicate this fact.

Received February 11, 2017; revised May 13, 2017; accepted June 20, 2017; published OnlineFirst June 26, 2017.

11. Hugo W, Zaretsky JM, Sun L, Song C, Moreno BH, Hu-Lieskovan S, et al. Genomic and transcriptomic features of response to anti-PD-1 therapy in metastatic melanoma. *Cell* 2016;165:35–44.
12. Hölzel M, Bovier A, Tüting T. Plasticity of tumour and immune cells: a source of heterogeneity and a cause for therapy resistance? *Nat Rev Cancer* 2013;13:365–76.
13. Müller J, Krijgsman O, Tsoi J, Robert L, Hugo W, Song C, et al. Low MITF/AXL ratio predicts early resistance to multiple targeted drugs in melanoma. *Nat Commun* 2014;5:5712.
14. Konieczkowski DJ, Johannessen CM, Abudayyeh O, Kim JW, Cooper ZA, Piris A, et al. A melanoma cell state distinction influences sensitivity to MAPK pathway inhibitors. *Cancer Discov* 2014;4:816–27.
15. Ramsdale R, Jorissen RN, Li FZ, Al-Obaidi S, Ward T, Sheppard KE, et al. The transcription cofactor c-JUN mediates phenotype switching and BRAF inhibitor resistance in melanoma. *Sci Signal* 2015;8:ra82.
16. Hoek KS, Eichhoff OM, Schlegel NC, Döbbeling U, Kobert N, Schaerer L, et al. In vivo switching of human melanoma cells between proliferative and invasive states. *Cancer Res* 2008;68:650–6.
17. Verfaillie A, Imrichova H, Atak ZK, Dewaele M, Rambow F, Hulselmans G, et al. Decoding the regulatory landscape of melanoma reveals TEADS as regulators of the invasive cell state. *Nat Commun* 2015;6:6683.
18. Tirosh I, Izar B, Prakadan SM, Wadsworth MH, Treacy D, Trombetta JJ, et al. Dissecting the multicellular ecosystem of metastatic melanoma by single-cell RNA-seq. *Science* 2016;352:189–96.
19. Gerber T, Willscher E, Loeffler-Wirth H, Hopp L, Schadendorf D, Scharlt M, et al. Mapping heterogeneity in patient-derived melanoma cultures by single-cell RNA-seq. *Oncotarget* 2016;8:846–62.
20. Landsberg J, Kohlmeyer J, Renn M, Bald T, Rogava M, Cron M, et al. Melanomas resist T-cell therapy through inflammation-induced reversible dedifferentiation. *Nature* 2012;490:412–6.
21. Riesenberger S, Groetchen A, Siddaway R, Bald T, Reinhardt J, Smorra D, et al. MITF and c-Jun antagonism interconnects melanoma dedifferentiation with pro-inflammatory cytokine responsiveness and myeloid cell recruitment. *Nat Commun* 2015;6:8755.
22. Hölzel M, Landsberg J, Glodde N, Bald T, Rogava M, Riesenberger S, et al. A Preclinical model of malignant peripheral nerve sheath tumor-like melanoma is characterized by infiltrating mast cells. *Cancer Res* 2016;76:251–63.
23. Hay CM, Sult E, Huang Q, Mulgrew K, Fuhrmann SR, McGlinchey KA, et al. Targeting CD73 in the tumor microenvironment with MEDI9447. *Oncoimmunology* 2016;5:e1208875.
24. Lin WM, Baker AC, Beroukhim R, Winckler W, Feng W, Marmion JM, et al. Modeling genomic diversity and tumor dependency in malignant melanoma. *Cancer Res* 2008;68:664–73.
25. Hölzel M, Tüting T. Inflammation-Induced Plasticity in Melanoma Therapy and Metastasis. *Trends Immunol* 2016;37:364–74.
26. Ohta A. A metabolic immune checkpoint: adenosine in tumor microenvironment. *Front Immunol* 2016;7:109.
27. Young A, Mittal D, Stagg J, Smyth MJ. Targeting cancer-derived adenosine: new therapeutic approaches. *Cancer Discov* 2014;4:879–88.
28. de Oliveira Bravo M, Carvalho JL, Saldanha-Araujo F. Adenosine production: a common path for mesenchymal stem-cell and regulatory T-cell-mediated immunosuppression. *Purinergic Signal* 2016;12:595–609.
29. Allard D, Allard B, Gaudreau P-O, Chrobak P, Stagg J. CD73-adenosine: a next-generation target in immuno-oncology. *Immunotherapy* 2016;8:145–63.
30. Young A, Ngoi SF, Barkauskas DS, Sult E, Hay C, Blake SJ, et al. Co-inhibition of CD73 and A2AR adenosine signaling improves anti-tumor immune responses. *Cancer Cell* 2016;30:391–403.
31. Weeraratna AT, Jiang Y, Hostetter G, Rosenblatt K, Duray P, Bittner M, et al. Wnt5a signaling directly affects cell motility and invasion of metastatic melanoma. *Cancer Cell* 2002;1:279–88.
32. Corso S, Giordano S. Cell-autonomous and non-cell-autonomous mechanisms of HGF/MET-driven resistance to targeted therapies: from basic research to a clinical perspective. *Cancer Discov* 2013;3:978–92.
33. Hodis E, Watson IR, Kryukov GV, Arold ST, Imielinski M, Theurillat J-P, et al. A landscape of driver mutations in melanoma. *Cell* 2012;150:251–63.
34. Wang H, Lee S, Nigro CL, Lattanzio L, Merlano M, Monteverde M, et al. NT5E (CD73) is epigenetically regulated in malignant melanoma and associated with metastatic site specificity. *Br J Cancer* 2012;106:1446–52.
35. Titz B, Lomova A, Le A, Hugo W, Kong X, Ten Hoeve J, et al. JUN dependency in distinct early and late BRAF inhibition adaptation states of melanoma. *Cell Discov* 2016;2:16028.
36. Wagner EF, Nebreda AR. Signal integration by JNK and p38 MAPK pathways in cancer development. *Nat Rev Cancer* 2009;9:537–49.
37. Uluçkan Ö, Guinea-Viniegra J, Jimenez M, Wagner EF. Signalling in inflammatory skin disease by AP-1 (Fos/Jun). *Clin Exp Rheumatol* 2015;33:S44–49.
38. Liberzon A, Birger C, Thorvaldsdóttir H, Ghandi M, Mesirov JP, Tamayo P. The molecular signatures database (MSigDB) hallmark gene set collection. *Cell Syst* 2015;1:417–25.
39. Widmer DS, Hoek KS, Cheng PF, Eichhoff OM, Biedermann T, Raaijmakers MIC, et al. Hypoxia contributes to melanoma heterogeneity by triggering HIF1 α -dependent phenotype switching. *J Invest Dermatol* 2013;133:2436–43.
40. O'Connell MP, Marchbank K, Webster MR, Valiga AA, Kaur A, Vultur A, et al. Hypoxia induces phenotypic plasticity and therapy resistance in melanoma via the tyrosine kinase receptors ROR1 and ROR2. *Cancer Discov* 2013;3:1378–93.
41. Hatfield SM, Kjaergaard J, Lukashev D, Belikoff B, Schreiber TH, Sethumadhavan S, et al. Systemic oxygenation weakens the hypoxia and hypoxia inducible factor 1 α -dependent and extracellular adenosine-mediated tumor protection. *J Mol Med Berl Ger* 2014;92:1283–92.
42. Hatfield SM, Kjaergaard J, Lukashev D, Schreiber TH, Belikoff B, Abbott R, et al. Immunological mechanisms of the antitumor effects of supplemental oxygenation. *Sci Transl Med* 2015;7:277ra30.
43. Allard B, Pommey S, Smyth MJ, Stagg J. Targeting CD73 enhances the antitumor activity of anti-PD-1 and anti-CTLA-4 mAbs. *Clin Cancer Res* 2013;19:5626–35.
44. Beavis PA, Milenkovski N, Henderson MA, John LB, Allard B, Loi S, et al. Adenosine receptor 2A blockade increases the efficacy of anti-PD-1 through enhanced antitumor T-cell Responses. *Cancer Immunol Res* 2015;3:506–17.
45. Iannone R, Miele L, Maiolino P, Pinto A, Morello S. Adenosine limits the therapeutic effectiveness of anti-CTLA4 mAb in a mouse melanoma model. *Am J Cancer Res* 2014;4:172–81.
46. Tume PC, Harview CL, Yearley JH, Shintaku IP, Taylor EJM, Robert L, et al. PD-1 blockade induces responses by inhibiting adaptive immune resistance. *Nature* 2014;515:568–71.
47. Sadej R, Spychala J, Skladanowski AC. Expression of ecto-5'-nucleotidase (eN, CD73) in cell lines from various stages of human melanoma. *Melanoma Res* 2006;16:213–22.
48. Falletta P, Sanchez-Del-Campo L, Chauhan J, Efferm M, Kenyon A, Kershaw CJ, et al. Translation reprogramming is an evolutionarily conserved driver of phenotypic plasticity and therapeutic resistance in melanoma. *Genes Dev* 2017;31:18–33.
49. Liu L, Mayes PA, Eastman S, Shi H, Yadavilli S, Zhang T, et al. The BRAF and MEK inhibitors dabrafenib and trametinib: effects on immune function and in combination with immunomodulatory antibodies targeting PD-1, PD-L1, and CTLA-4. *Clin Cancer Res* 2015;21:1639–51.
50. Bald T, Quast T, Landsberg J, Rogava M, Glodde N, Lopez-Ramos D, et al. Ultraviolet-radiation-induced inflammation promotes angiogenesis and metastasis in melanoma. *Nature* 2014;507:109–13.
51. Braumüller H, Wiedner T, Brenner E, Afsmann S, Hahn M, Alkhaled M, et al. T-helper-1-cell cytokines drive cancer into senescence. *Nature* 2013;494:361–5.
52. Benci JL, Xu B, Qiu Y, Wu TJ, Dada H, Twyman-SaintVictor C, et al. Tumor interferon signaling regulates a multigenic resistance program to immune checkpoint blockade. *Cell* 2016;167:1540–54.
53. Spranger S, Gajewski T. Rational combinations of immunotherapeutics that target discrete pathways. *J Immunother Cancer* 2013;1:16.
54. Deaglio S, Dwyer KM, Gao W, Friedman D, Usheva A, Erat A, et al. Adenosine generation catalyzed by CD39 and CD73 expressed on regulatory T cells mediates immune suppression. *J Exp Med* 2007;204:1257–65.
55. Beavis PA, Stagg J, Darcy PK, Smyth MJ. CD73: a potent suppressor of antitumor immune responses. *Trends Immunol* 2012;33:231–7.

Cancer Research

The Journal of Cancer Research (1916–1930) | The American Journal of Cancer (1931–1940)

MAPK Signaling and Inflammation Link Melanoma Phenotype Switching to Induction of CD73 during Immunotherapy

Julia Reinhardt, Jennifer Landsberg, Jonathan L. Schmid-Burgk, et al.

Cancer Res 2017;77:4697-4709. Published OnlineFirst June 26, 2017.

Updated version Access the most recent version of this article at:
doi:[10.1158/0008-5472.CAN-17-0395](https://doi.org/10.1158/0008-5472.CAN-17-0395)

Supplementary Material Access the most recent supplemental material at:
<http://cancerres.aacrjournals.org/content/suppl/2017/06/24/0008-5472.CAN-17-0395.DC1>

Cited articles This article cites 55 articles, 19 of which you can access for free at:
<http://cancerres.aacrjournals.org/content/77/17/4697.full#ref-list-1>

Citing articles This article has been cited by 2 HighWire-hosted articles. Access the articles at:
<http://cancerres.aacrjournals.org/content/77/17/4697.full#related-urls>

E-mail alerts [Sign up to receive free email-alerts](#) related to this article or journal.

Reprints and Subscriptions To order reprints of this article or to subscribe to the journal, contact the AACR Publications Department at pubs@aacr.org.

Permissions To request permission to re-use all or part of this article, use this link
<http://cancerres.aacrjournals.org/content/77/17/4697>.
Click on "Request Permissions" which will take you to the Copyright Clearance Center's (CCC) Rightslink site.